N-Terminal Sugar Conjugation and C-Terminal Thr-for-Thr(ol) Exchange in Radioiodinated Tyr^3-octreotide: Effect on Cellular Ligand Trafficking in Vitro and Tumor Accumulation in Vivo

Margret Schottelius,*,† Jean Claude Reubi,‡ Veronique Eltschinger,‡ Markus Schwaiger,† and Hans-Jürgen Wester†

Nuklearmedizinische Klinik und Poliklinik, Klinikum rechts der Isar, Technische Universität München, 81675 München, Germany, and Institut für Pathologie, Universität Bern, 3010 Bern, Switzerland

Received February 23, 2004

For effective targeting of somatostatin receptor (sst) expressing tumors by radiolabeled octreotide analogues, high ligand uptake into sst-positive cells is mandatory. To optimize it, two modifications have been introduced into [^{125}I]Tyr^3-octreotide ([^{125}I]TOC): C-terminal Thr-for-Thr(ol) exchange (leading to Tyr^3-octreotate (TOCA)) and N-terminal derivatization with different carbohydrates. Both have significant impact on radioligand uptake into sst$_2$-expressing cells in vitro and in vivo. Glucose conjugation via Amadori reaction by itself led to improved tumor uptake of [^{123}I]Gluc-TOC in vivo, which is based on an enhancement of peptide internalization despite a reduction in receptor affinity. In the case of the doubly modified analogues [^{123}I]Gluc-TOCA, [^{123}I]Gluc-*S*-TOCA, and [^{123}I]Gal-*S*-TOCA, a cumulative effect of both structural modifications was observed, leading up to a 5-fold increased uptake of these compounds in sst-expressing tumors compared to [^{125}I]TOC. Thus, glycosylation with small carbohydrates was found to be a suitable tool to enhance receptor-mediated uptake of radiolabeled octreotide analogues into sst-positive malignancies, leading to tracers with excellent characteristics for in vivo sst-imaging applications.

Introduction

A variety of human tumors overexpress high-affinity receptors for small peptide hormones such as somatostatin (sst),[1] vasoactive intestinal peptide (VPAC),[2−4] neurotensin (NT),[5] substance P,[6] gastrin-releasing peptide (GRP),[7] cholecystokinin (CCK),[8] oxytocin,[9,10] vasopressin,[11] and α-melanocyte stimulating hormone (α-MSH),[12] providing the opportunity for in vivo receptor scintigraphy and endoradiotherapy with radiolabeled neuropeptides. So far, only somatostatin receptor ligands such as [^{111}In]octreoscan[13,14] or [^{90}Y]DOTATOC[15−17] have found widespread application in nuclear oncology. In recent years, however, intensive research has been directed toward the optimization of other radiolabeled neuropeptide receptor ligands with respect to labeling methodology, in vivo stability, and pharmacokinetic properties, yielding promising candidates for in vivo VPAC,[18] NT,[19] GRP, and CCK[20−23] receptor imaging.

Generally, the targeting efficiency of neuropeptide analogues to tumor cells relies on the overexpression of their cognate receptors on the cell surface as well as on the extent of their internalization into receptor-expressing cells. The latter process is of particular relevance for in vivo tumor targeting, since it leads to intracellular accumulation of the radionuclide and thus enhances the scintigraphic signal and/or the therapeutic ratio. Because of their predominant clinical role, the internalization of radiolabeled somatostatin analogues into sst-receptor expressing cells and the subsequent intracellular trafficking of both receptor and ligand has been extensively studied.[24,25]

Upon ligand binding, all five human somatostatin receptor subtypes (hsst$_{1-5}$) are internalized in a time-, temperature-, and subtype-dependent manner (hsst$_3$ > hsst$_5$ > hsst$_4$ > hsst$_2$ > hsst$_1$).[26]

The amount of internalized receptor−agonist complex can be influenced by the level of cellular receptor regulation[27,28] and by the structure of the radioligand. The latter has been demonstrated by Koenig et al., who found substantially increased internalization of the synthetic somatostatin analogue [^{125}I]BIM-23027 compared to that of [^{125}I]SRIF-14 in CHO cells stably transfected with hsst$_2$, suggesting that the structure of the radioligand may have a significant impact on the extent of endocytosis.[24] Furthermore, comparative studies revealed that internalization of radiolabeled octreotide analogues can be substantially increased by Tyr^3-for-Phe^3 substitution and even more so by C-terminal Thr(ol)^8-for-Thr^8 exchange.[29,30] This finding constitutes the basis of endoradiotherapeutic strategies applying Tyr^3-octreotate (TOCA) analogues labeled with low-energy β emitters such as ^{153}Sm [31] and ^{177}Lu.[32,33] Despite comparably lower internalization, promising therapeutic results have also been obtained in clinical studies with [^{111}In]DTPA-octreotide.[34,35] The success of these endoradiotherapeutic strategies, especially when low-energy particle emitting radionuclides are applied, crucially depends on the amount of radioligand accumulated inside the tumor cells.

This quantity, however, is determined not only by the extent of ligand internalization but also by the rates of externalization, recycling, and/or degradation of both

* To whom correspondence should be addressed. Phone: 49 89 4140 4554/6340. Fax: 49 89 4140 4897. E-mail: M.Schottelius@lrz.tum.de.
† Technische Universität München.
‡ Universität Bern.

10.1021/jm040794i CCC: $30.25
Published on Web 03/01/2005

radioligand and receptor. Both the somatostatin receptor[25] and associated ligands[24] were shown to be mainly externalized after dissociation of the receptor−ligand complex in the early endosomal compartment. While the rate of externalization of intact radioligand was found to be agonist-independent, the degree of ligand degradation and particularly of intracellular activity retention strongly depends on the nature of the radioligand used and on the radiolabeling method.[24] Radioiodinated SRIF-14 showed rapid and extensive intracellular degradation and subsequent release of [^{125}I]iodotyrosine into the external medium,[24] whereas radiometalated octreotide analogues showed significantly reduced intracellular degradation rates. However, substantial residualization of radioactivity inside the cells after longer incubation times (~40 h)[36] has been observed, which has been explained by the trapping of the charged radiometal-chelate-containing fragments in the lysosomal compartments.[37,38]

In previous studies, we have investigated the effect of N-terminal glycosylation of ^{125}I-,[39−41] ^{111}In-,[42] ^{99m}Tc-,[43] and ^{18}F-labeled[44,45] octreotide and/or octreotate derivatives on their pharmacokinetics and tumor accumulation in vivo. Biodistribution studies in AR42J tumor-bearing nude mice showed that glucose conjugation of radioiodinated Tyr^3-octreotide (TOC) leads to increased tumor accumulation.[39] Furthermore, the combination of C-terminal substitution of Thr(ol) by Thr with sugar derivatization as in [^{123}I]maltotriose octreotate ([^{123}I]Mtr-TOCA) was shown to yield radioiodinated somatostatin analogues with excellent excretion characteristics and high tumor accumulation suitable for in vivo sst receptor imaging.[40] Recently, initial patient PET studies were performed using [^{18}F]Gluc-Lys(FP)-TOCA for the localization of sst-positive tumors.[44] As found for [^{123}I]Mtr-TOCA, very high tumor-to-background ratios were obtained at early time points (<60 min) with negligible accumulation in excretion organs, demonstrating the compatibility of the "glycosylated octreotate" concept with different labeling methodologies.

To quantify the effects of glycosylation and C-terminal Thr(ol)-by-Thr substitution on ligand uptake into sst-expressing tissues on a cellular level, we performed detailed in vitro studies with two series of radioiodinated, glycosylated TOC-analogues: [^{125}I]TOC and its glucose- ([^{123}I]Gluc-TOC) , maltose- ([^{123}I]Malt-TOC), and maltotriose- ([^{123}I]Mtr-TOC) Amadori derivatives as well as [^{123}I]TOCA and its corresponding sugar analogues [^{123}I]Gluc-TOCA, [^{123}I]Malt-TOCA, and [^{123}I]Mtr-TOCA. Additionally, the effect of an alternative glycosylation method via a mercaptopropionic acid linker was investigated using [^{123}I]Gluc-*S*-TOCA and [^{123}I]Gal-*S*-TOCA (Figure 1).

Three major determinants for radioligand accumulation in tumor cells were investigated: (a) the sst-receptor affinity and specificity, (b) the internalization, and (c) the extent of ligand externalization and recycling. Additionally, the EC_{50} of unlabeled TOC for ligand internalization was determined for all compounds investigated. Experiments were performed as dual tracer experiments (^{123}I-labeled compound of interest + [^{125}I]TOC as an internal reference) both in CHO (chinese hamster ovary) cells stably transfected with $hsst_2$

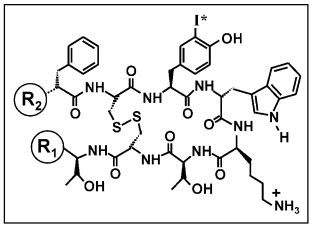

1A [*I]TOC: R_1 = CH_2OH R_2 = $\overset{+}{N}H_3$

2A [*I]TOCA: R_1 = COOH R_2 = $\overset{+}{N}H_3$

1B [*I]Gluc-TOC: R_1 = CH_2OH

2B [*I]Gluc-TOCA: R_1 = COOH

R_2 =

1C [*I]Malt-TOC: R_1 = CH_2OH

2C [*I]Malt-TOCA: R_1 = COOH

R_2 =

1D [*I]Mtr-TOC: R_1 = CH_2OH

2D [*I]Mtr-TOCA: R_1 = COOH

R_2 =

2E [*I]Gluc-*S*-TOCA: R_1 = COOH R_2 =

2F [*I]Gal-*S*-TOCA: R_1 = COOH R_2 =

Figure 1. Structure of the carbohydrate analogues of radioiodinated TOC and TOCA investigated in this study.

(epitope tagged at the N-terminal end) and in the rat pancreatic tumor cell line AR42J.

Results

Peptide Synthesis. Solid-phase peptide synthesis (SPPS) of TOC(Dde), I-TOC(Dde), TOCA(Dde), and I-TOCA(Dde) was carried out using a standard Fmoc protocol and HOBt and TBTU as coupling agents. Yields ranged from 85% to 97% based on resin-bound amino acid or alcohol. Cyclization of the freshly cleaved peptides using H_2O_2 in an aqueous THF solution buffered to pH 7 proceeded smoothly within less than 30 min. While UV purities (220 nm) of crude cyclized TOC(Dde) and TOCA(Dde) usually exceeded 93%, more side products were observed for both 3-iodo-Tyr^3-containing peptides (up to 20%). However, all peptides were used for the following reaction steps without further purification.

The N-terminal glycosylation of the parent peptides with glucose, maltose, or maltotriose was achieved within 16−20 h in yields up to 85% (value based on the integration of product and precursor peaks in the reaction control RP-HPLC chromatograms (220 nm)).

Synthesis of the pentafluorophenyl esters of 1-*S*(2,3,4,6-tetraacetylglucopyranosyl)-3-mercaptopropionate and the corresponding galactose analogue from the peracetylated sugar precursors was achieved in two steps in 68−78% overall yield. In contrast to the long reaction times and elevated temperatures needed for Amadori glycosylation, N-terminal conjugation of TOCA(Dde) with the aforementioned thioglycoside active esters was quantitative within 30−45 min at room temperature.

After subsequent Dde deprotection (and deacetylation in the case of Gluc-*S*- and Gal-*S*-TOCA) and preparative RP-HPLC purification, all glycosylated TOC and TOCA derivatives as well as their 3-iodo-Tyr^3 counterparts

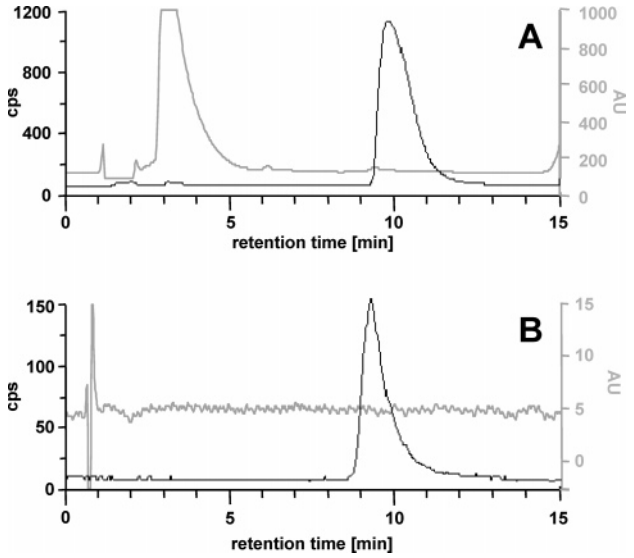

Figure 2. Preparative RP-HPLC (A, isocratic eluent of 28% EtOH (0.5% AcOH) in water (0.5% AcOH)) and analytical quality control chromatogram (B, isocratic eluent of 29% EtOH (0.5% AcOH) in water (0.5% AcOH)) of [^{125}I]TOC.

were obtained in purities of ≥98%. Overall yields of all glycosylated peptides based on nonglycosylated precursor ranged from 15% to 34%.

Radiolabeling. The efficiency of radioiodide incorporation usually exceeded 95%. However, because of the formation of radioiodinated side products, radiochemical yields of the ^{125}I- and ^{123}I-labeled peptides after RP-HPLC isolation only ranged from 45% to 85%. All radioiodinated peptides were obtained in high radiochemical purity (>99%).

Since the HPLC conditions applied allowed very efficient separation of the radioiodinated product from the unlabeled precursor (as shown for [^{125}I]TOC in Figure 2, $\Delta t_R \geq 5$ min) for all radioligands investigated and since no coeluting carrier peak was observed in the labeled peptide peak on the quality control UV chromatogram, the specific activity of the labeled peptides was assumed to be that of the radioiodide used for their preparation (≥74 GBq/μmol for ^{125}I, ~185 GBq/μmol for ^{123}I).

Affinity Profiles to hsst. In vitro binding properties of I-TOC, I-TOCA, and their corresponding carbohydrated analogues were investigated using cells stably expressing sst_1−sst_5 in displacement experiments using [^{125}I][Leu^8,D-Trp^{22},Trp^{25}]somatostatin 28 as radioligand. Results are summarized in Table 1 and are compared to the control peptide native somatostatin 28, which binds with high affinity to all five sst subtypes.

All octreotide analogues investigated showed no affinity to sst_1, very high affinity to sst_2, and moderate or low affinity to sst_{3-5}. Generally, substitution of Thr(ol)^8 by Thr^8 (I-TOC → I-TOCA) resulted in an increase in sst_2 and sst_4 affinity. The N-terminal glycosylation led to decreased sst_2 affinities (except I-Malt-TOC and I-Mtr-TOC) and sst_3 affinities compared to nonmodified I-TOC and I-TOCA, respectively. Moreover, all sugar analogues of I-TOCA, independent of the glycosylation method, showed decreased sst_3 and sst_5 affinity compared to their corresponding I-TOC-counterparts and thus enhanced sst_2 specificity. Of the compounds investigated, I-Malt-TOCA and I-Mtr-TOCA demonstrated the highest sst_2 specificity.

Internalization and $EC_{50,R}$ in CHO Cells. The amount of internalized [^{123}I]Gluc-TOC, [^{123}I]Malt-TOC, and [^{123}I]Mtr-TOC and of [^{123}I]TOCA and its five sugar analogues into CHO cells normalized to the value found for [^{125}I]TOC from the same experiment in the absence of unlabeled competitor is shown in Figure 3. While conjugation of [^{125}I]TOC with maltose and maltotriose had a comparably small effect on ligand internalization (109.7 ± 5.5% for [^{123}I]Malt-TOC and 93.0 ± 5.0% for [^{123}I]Mtr-TOC), the internalization of [^{123}I]Gluc-TOC was increased by 28.8 ± 9.4% compared to that of [^{125}I]TOC. For [^{123}I]TOCA, a significant increase in ligand internalization due to C-terminal Thr^8-for-Thr(ol)^8 exchange was found (178.8 ± 6.9% of [^{125}I]TOC). As observed for [^{125}I]TOC, both the maltose and maltotriose derivatives as well as the Gal-*S* derivative of [^{125}I]TOCA also showed nearly unchanged internalization compared to their nonmodified analogue. [^{123}I]Gluc-TOCA, however, showed higher internalization than [^{125}I]TOCA (193.1 ± 12.4% of [^{125}I]TOC). For [^{123}I]Gluc-*S*-TOCA, the highest internalization among the com-

Table 1. Affinity Profiles (IC_{50}) to the Human sst_{1-5} Receptors Determined for Somatostatin 28 (SS 28) and the Compounds Investigated Using [^{125}I][Leu^8,D-Trp^{22},Tyr^{25}]Somatostatin 28 as the Radioligand (Values Are IC_{50} ± SD [nM], and Number of Experiments Are in Parentheses)[a]

peptide	$hsst_1$	$hsst_2$	$hsst_3$	$hsst_4$	$hsst_5$
SS-28	3.6 ± 0.3 (5)	2.1 ± 0.3 (5)	3.2 ± 0.2 (5)	3 ± 0.3 (5)	2.5 ± 0.2 (5)
TOC	>1000 (2)	3.1 ± 1.8 (2)	330 ± 146 (2)	346 ± 114 (2)	10.8 ± 1.8 (2)
I-TOC	>1000 (5)	1.6 ± 0.4 (5)	186 ± 52 (5)	729 ± 87 (5)	65 ± 17 (5)
I-Gluc-TOC	>1000 (3)	2.2 ± 0.7 (3)	357 ± 22 (3)	837 ± 154 (3)	64 ± 24 (3)
I-Malt-TOC	>10000 (3)	1.2 ± 0.2 (3)	243 ± 47 (3)	>1000 (3)	75 ± 19 (3)
I-Mtr-TOC	>10000 (3)	1.1 ± 0.2 (3)	210 ± 15 (3)	>1000 (3)	110 ± 35 (3)
I-TOCA	>10000 (3)	0.47 ± 0.2 (3)	187 ± 38 (3)	337 ± 57 (3)	50 ± 5.8 (3)
I-Gluc-TOCA	>1000 (3)	2.0 ± 0.5 (3)	>1000 (3)	1033 ± 142 (3)	521 ± 269 (3)
I-Malt-TOCA	>10000 (3)	0.78 ± 0.2 (3)	757 ± 169 (3)	797 ± 61 (3)	210 ± 46 (3)
I-Mtr-TOCA	>10000 (3)	0.95 ± 0.3 (3)	823 ± 67 (3)	823 ± 87 (3)	327 ± 93 (3)
I-Gluc-*S*-TOCA	>1000 (3)	2.0 ± 0.7 (3)	398 ± 19 (3)	356 ± 60 (3)	310 ± 156 (3)
I-Gal-*S*-TOCA	>1000 (3)	2.0 ± 0.8 (3)	491 ± 63 (3)	482 ± 134 (3)	413 ± 167 (3)
DOTA-TOC[b]	>10000 (7)	14 ± 2.6 (6)	880 ± 324 (4)	>1000 (6)	393 ± 84 (6)
DOTA-TOCA[b]	>10000 (3)	1.5 ± 0.4 (3)	>1000 (3)	453 ± 176 (3)	547 ± 160 (3)
Y-DOTA-TOC[b]	>10000 (4)	11 ± 1.7 (6)	389 ± 135 (5)	>10000 (5)	114 ± 29 (5)
Y-DOTA-TOCA[b]	>10000 (3)	1.6 ± 0.4 (3)	>1000 (3)	523 ± 239 (3)	187 ± 50 (3)
Ga-DOTA-TOC[b]	>10000 (6)	2.5 ± 0.5 (7)	613 ± 140 (7)	>1000 (6)	73 ± 21 (6)
Ga-DOTA-TOCA[b]	>10000 (3)	0.2 ± 0.04 (3)	>1000 (3)	300 ± 140 (3)	377 ± 18 (3)

[a] Cell membrane pellets were prepared from CHO-K1 cells (sst_1 and sst_5) and CCL39 cells (sst_{2-4}).[48] [b] Cited from ref 48.

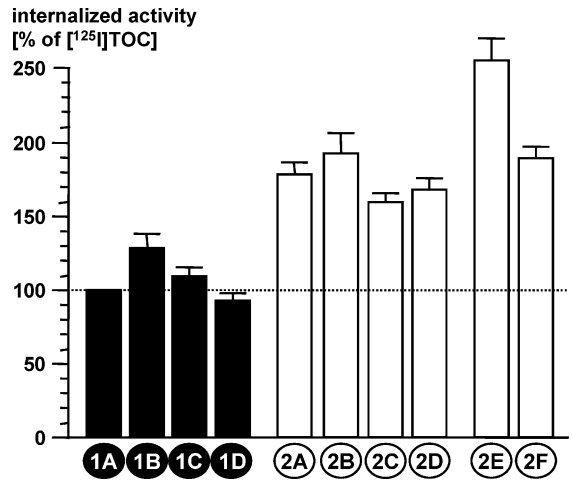

Figure 3. Internalization of peptides **1B**−**2F** in CHO cells ($hsst_2$) as percent of the internalization of the reference [^{125}I]-TOC (**1A**) found in the same experiment (mean ± SD; $n = 3$ in two (∗) or three separate determinations, 10 min incubation).

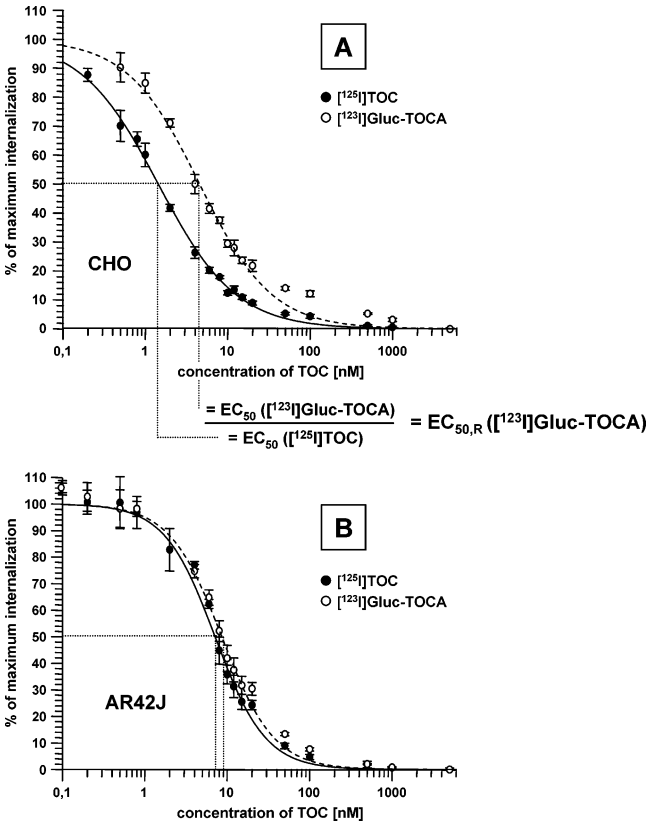

Figure 4. Determination of the EC_{50} of unlabeled TOC for the internalization of [^{125}I]TOC (full circles) and [^{123}I]Gluc-TOCA (hollow circles) in CHO ($hsst_2$) (A) and AR42J ($rsst_2$) (B) cells (data are the mean ± SD; $n = 3$) and calculation of the $EC_{50,R}$ for [^{123}I]Gluc-TOCA.

pounds investigated in this study was found (264.7 ± 20.3% of [^{125}I]TOC).

The $EC_{50,R}$ values obtained for [^{125}I]TOC, [^{123}I]TOCA, and their corresponding glucose, maltose, and maltotriose conjugates using CHO cells (Figure 4 A) are summarized in Table 2. In both the [^{125}I]TOC and the [^{123}I]TOCA series, the same pattern in the $EC_{50,R}$ was found: Gluc > Malt > Mtr ∼ nonglycosylated analogue. For all [^{123}I]TOCA derivatives, values were significantly higher than those found for their corresponding

Table 2. Relative EC_{50} Values ($EC_{50,R}$) for the Internalization of Glycosylated [^{123}I]TOC and [^{123}I]TOCA Derivatives Determined Using CHO Cells Stably Expressing $hsst_2$ ($n = 3$ in Two (∗) or Three Separate Determinations, Mean ± SD)

	$EC_{50,R}$
[^{125}I]TOC	1
[^{123}I]Gluc-TOC	1.43 ± 0.06
[^{123}I]Malt-TOC*	1.12 ± 0.05
[^{123}I]Mtr-TOC*	1.01 ± 0.12
[^{123}I]TOCA	1.70 ± 0.11
[^{123}I]Gluc-TOCA	2.51 ± 0.12
[^{123}I]Malt-TOCA	2.13 ± 0.19
[^{123}I]Mtr-TOCA	1.81 ± 0.07
[^{123}I]Gluc-*S*-TOCA	2.96 ± 0.14
[^{123}I]Gal-*S*-TOCA	2.62 ± 0.07

Thr(ol)[8] counterparts ($P < 0.001$). Of the Amadori analogues investigated, [^{123}I]Gluc-TOCA had the highest $EC_{50,R}$. Both thioglycoside-modified TOCA analogues, however, showed even higher $EC_{50,R}$ values of up to 2.96 ± 0.14 ([^{123}I]Gluc-*S*-TOCA).

Externalization and Recycling in CHO Cells. To assess the extent of ligand externalization of the carbohydrated [^{123}I]TOC and [^{123}I]TOCA analogues from CHO cells compared to [^{125}I]TOC and to investigate the role of ligand recycling (reuptake after externalization), two experiments were performed. After an initial incubation for 10 min, allowing the internalization of the radioligands, cells were washed and then incubated with radioligand-free medium containing either no unlabeled competitor (conditions allowing recycling) or 5 μM TOC (conditions inhibiting recycling) for 30 and 60 min. To ensure receptor integrity, no acid wash was performed after the internalization incubation. Thus, externalization data are given as the percent of the cellularly located activity (internalized + receptor bound) at $t = 0$ of the externalization incubation.

Figure 5A depicts a typical externalization profile of a glycosylated *I-TOC-analogue compared to [^{125}I]TOC, in this case shown for [^{123}I]Gluc-TOCA. Both under conditions allowing and inhibiting ligand recycling, all glycosylated [^{125}I]TOC and [^{123}I]TOCA analogues showed nearly identical externalization profiles (data not shown). When ligand recycling was allowed, 90−93% of the cellular radioactivity at $t = 0$ were still found inside the cells after 30 min ([^{125}I]TOC: 82−86%) for all sugar analogues. After 60 min, the amount of intracellularly located radioactivity was reduced to 82−86% of the initial activity in the case of the carbohydrated peptides analogues and to 79−83% for [^{125}I]TOC. Under conditions inhibiting recycling, only 4−8% of the initial cellularly located radioactivity was found to remain internalized after 60 min for all carbohydrated peptides as well as for the reference [^{125}I]TOC.

Internalization and $EC_{50,R}$ in AR42J Cells. To investigate to what extent the internalization of glycosylated [^{125}I]TOC analogues is dependent on the cell line used, a comparative EC_{50} determination was performed in AR42J cells using [^{123}I]Gluc-TOCA as an exemplary carbohydrated radioligand (Figure 4B). In AR42J-cells, [^{123}I]Gluc-TOCA showed 277.9 ± 10.5% of the internalization found for [^{125}I]TOC (vs 193.1 ± 12.4% in CHO cells). However, the $EC_{50,R}$ found for [^{123}I]Gluc-TOCA in AR42J cells was unexpectedly low (1.14 ± 0.04 vs 2.51 ± 0.12 in CHO cells).

Externalization and Recycling in AR42J Cells. The externalization of [^{123}I]Gluc-TOCA from AR42J cells

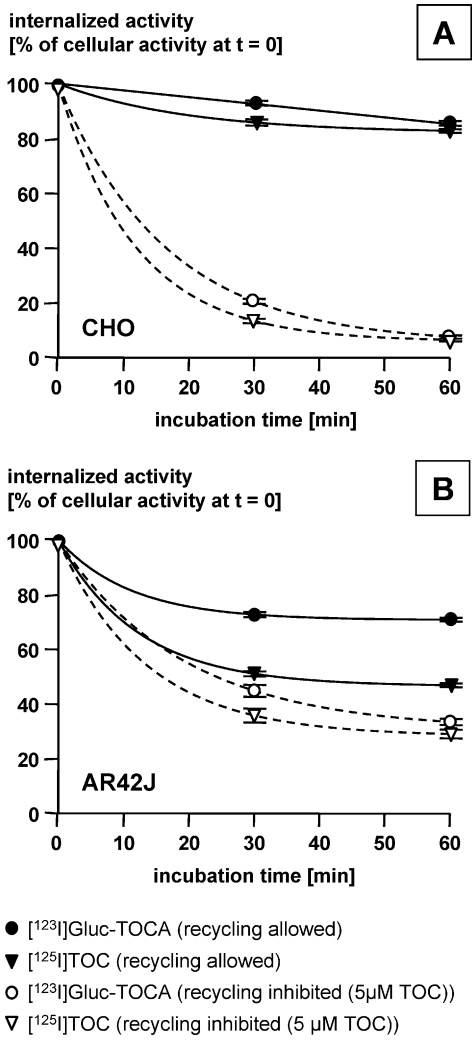

Figure 5. Externalization kinetics of [^{123}I]Gluc-TOCA (circles) and [^{125}I]TOC (down triangles) under conditions allowing (ligand-free medium; solid icons, solid lines) and inhibiting (5 μM TOC; hollow icons, dashed lines) ligand recycling in CHO ($hsst_2$) (A) and AR42J ($rsst_2$) (B) cells. Data are given as percent of the cellularly located activity (internalized + receptor bound ligand) at $t = 0$ of the externalization experiment (after a 10 min internalization incubation). Data are the mean ± SD ($n = 3$).

compared to the externalization from CHO cells is shown in Figure 5B. Under conditions allowing ligand recycling, 72.6 ± 0.9% and 70.8 ± 0.3% of the cellularly located activity ($t = 0$) remained internalized in the case of [^{123}I]Gluc-TOCA after 30 and 60 min, respectively. For [^{125}I]TOC, only 51.1 ± 1.0% and 46.9 ± 0.3% of the initial activity were found inside the cells. When ligand recycling was inhibited by 5 μM TOC, however, the fraction of both [^{123}I]Gluc-TOCA and [^{125}I]TOC remaining internalized after 60 min was, like in CHO cells, comparable ([^{123}I]Gluc-TOCA, 33.4 ± 1.2%; [^{125}I]TOC, 29.1 ± 1.6%). However, in contrast to the data obtained with CHO cells (4−8%), a significantly higher amount of activity remained inside the AR42J cells under these conditions.

Tumor Accumulation in Vivo. Tumor accumulation of [^{125}I]TOC, [^{125}I]TOCA, and their respective sugar conjugates in nude mice bearing AR42J tumor with high sst_2 expression 60 min p.i. is summarized in Table 3. As observed in the internalization studies, Thr^8-for-Thr(ol)^8 exchange (TOC → TOCA) resulted in dramatically increased uptake of the radioligands in sst-expressing tumor tissue. In the [^{125}I]TOC series, only glucose conjugation led to a significant increase in tumor uptake of approximately 160% ($P < 0.001$), while the [^{125}I]Malt-TOC and [^{125}I]Mtr-TOC showed an accumulation comparable to [^{125}I]TOC. In contrast, in the [^{125}I]TOCA-series, [^{125}I]Gluc-TOCA showed a tumor uptake comparable to that of [^{125}I]TOCA, whereas tumor accumulation of [^{125}I]Mtr-TOCA was higher. Of all sugar analogues of [^{125}I]TOCA investigated, [^{125}I]Gluc-*S*-TOCA showed the highest uptake in sst-expressing tumor tissue.

Table 3. In Vivo Tumor Accumulation of [^{125}I]TOC, [^{125}I]TOCA, and Their Glycosylated Analogues in AR42J Tumor-Bearing Nude Mice 60 min p.i. (∗, 30 min p.i.)[a]

	tumor accumulation [% ID/g]
[^{125}I]TOC	5.5 ± 1.1
[^{123}I]Gluc-TOC	8.7 ± 1.5
[^{123}I]Malt-TOC	5.2 ± 0.6
[^{123}I]Mtr-TOC*	4.9 ± 2.2
[^{123}I]TOCA	21.2 ± 9.7
[^{123}I]Gluc-TOCA	20.5 ± 11.1
[^{123}I]Malt-TOCA	11.2 ± 2.4
[^{123}I]Mtr-TOCA	25.1 ± 4.4
[^{123}I]Gluc-*S*-TOCA	26.2 ± 7.5
[^{123}I]Gal-*S*-TOCA	22.6 ± 2.2

[a] Data are % ID/g ($n = 3$−5, mean ± SD).

Discussion

In Figure 1, the structures of radioiodinated TOC and TOCA and their respective analogues obtained from the Amadori reaction with glucose (Gluc-TOC/TOCA), maltose (Malt-TOC/TOCA), and maltotriose (Mtr-TOC/TOCA) are shown. It is important to note that only one of four possible conformations of the sugar moiety is shown. Besides the β-pyranoid structure (Figure 1), the α- and β-furanoid and the open-chain conformations of the deoxyketoses are possible and may be present in equilibrium mixtures.[46] However, during preparative and analytical RP-HPLC using isocratic conditions, only one peak was observed for all Amadori compounds (data not shown). Therefore, it seems probable that in the case of all Amadori analogues one sugar conformer represents the predominant species.

The major advantage of glycosylation via thioglycoside conjugation versus Amadori reaction consists of the known conformation of the sugar residue in [^{125}I]Gluc- and [^{125}I]Gal-*S*-TOCA. As determined by ^{1}H NMR, only the β-thioglycoside is produced during the reaction between the sugar 1,2-trans peracetate precursors and 3-mercaptopropionic acid. Furthermore, compared to glycosylation via Amadori reaction, peptide acylation with S-glycosylated 3-mercaptopropionic acid results in a much greater ease of synthesis, i.e., shorter reaction times (30 min vs 16 h), higher glycosylation yields (>99% vs ∼80%) and a significantly lower proportion of side product formation.

For the in vitro assays, the experimental setup chosen for the comparative evaluation of the carbohydrated [^{123}I]TOC and [^{123}I]TOCA derivatives was modified compared to previous studies. In earlier internalization experiments with AR42J cells,[47] both the compound of interest and the reference TOC had been labeled with iodine-125 and assayed in separate wells. Under these

conditions, limited reproducibility of the internalization data (i.e., internalization of the compound of interest as the percent of the internalization found for [^{125}I]TOC in the same experiment) was found. Small variations in the specific activities of the compared compounds as well as differences in cell count and cell viability between wells might have been responsible for the discrepancy in the outcome of the experiments. To eliminate these potential sources of error, a dual-tracer protocol was established. In the experiments performed in this study, cells were always coincubated with the ^{123}I-labeled compound of interest and the reference compound [^{125}I]TOC. This experimental setup guarantees identical (radio)ligand concentrations in all wells and additionally eliminates potential effects of cell count and cell viability on the internalization data.

The experiments were carried out using two different cell lines, CHO cells stably transfected with hsst$_2$ and AR42J rat pancreatic tumor cells endogenously expressing rsst$_2$. Since the rate and extent of ligand accumulation (per 100 000 cells) into the cells varies significantly between these cell lines, experimental conditions were adjusted such that for both cell lines absolute uptake of the reference [^{125}I]TOC ranged between 15% and 20% of the applied activity. While an incubation time of only 10 min was sufficient to achieve this in the case of the CHO cells (approximately 100 000 cells per well), AR42J cells (approximately 250 000 cells per well) required an incubation time of 30 min to obtain comparable intracellular activity levels. This adjustment of conditions ensures comparability of data between the cell lines, since consequently radioligand concentrations in the internalization medium were comparable for both cell lines.

As expected from previous findings with radiometal-labeled sst ligands (Table 1),[48] in vitro sst$_2$ affinity of [^{125}I]TOC was markedly improved by C-terminal Thr(ol)-by-Thr substitution leading to [^{125}I]TOCA, whereas affinity to all other sst subtypes remained nearly unaffected by this modification. The improvement of sst$_2$ affinity of [^{125}I]TOCA vs [^{125}I]TOC by a factor of ~3, however, was not as drastic as observed for the respective radiometalated and nonradiometalated DOTA analogues (factor of up to 10). As anticipated for the N-terminal introduction of a relatively bulky residue and as already demonstrated for the modification of TOC with DOTA, carbohydration of [^{125}I]TOC and more notedly of [^{125}I]TOCA generally led to reduced sst$_2$ affinity (Table 1). Interestingly, this effect was more pronounced in the case of the monosaccharides Gluc- ($P < 0.001$) as well as Gluc-*S*- ($0.001 < P < 0.0027$) and Gal-*S*- ($P < 0.001$) than in the case of the even bulkier di- and trisaccharides Malt- and Mtr- ($0.01 < P < 0.1$).

Basically, all tested compounds with a high sst$_2$ affinity also showed a high internalization rate. Within this group of rapidly internalized compounds with very high sst$_2$ affinity, one can, however, observe that the amount of glycosylated radioligand internalized into sst$_2$-expressing CHO cells (as percent of the reference [^{125}I]TOC) (Figure 3) does not necessarily correlate with their respective binding affinity to hsst$_2$ (Table 1). Some previous studies have also demonstrated that octreotide analogues with comparable binding affinity exhibited considerable differences in internalization efficiency.[28,29,49] Of the compounds investigated, those with the lowest sst$_2$ affinity compared to their non-carbohydrated counterparts showed the highest increase in internalization, namely, [^{123}I]Gluc-TOC (in the TOC series) and [^{123}I]Gluc-TOCA, [^{123}I]Gluc-*S*-TOCA, and [^{123}I]Gal-*S*-TOCA (in the TOCA series). In the case of the TOCA analogues, a cumulation of the effects of glycosylation and C-terminal Thr(ol)-by-Thr substitution on internalization was observed. Thus, conjugation with small sugar residues, independent of the presence or absence of a linker unit between peptide and sugar, substantially enhances internalization of the sst ligands investigated, whereas larger carbohydrates such as maltose and maltotriose do not trigger the same effect.

It might be assumed that variations in agonistic potency among the peptides modified with mono- versus di- or trisaccharides may be responsible for the above observation. In a previous study, however, a variety of Amadori analogues of octreotide (OC) including the Gluc, Malt, and Mtr derivatives have been evaluated.[50] While the receptor affinity of the peptides decreased only marginally in the order Gluc-OC > OC > Mtr-OC > Malt-OC, the IC$_{50}$ [nM] of the peptides for in vitro growth hormone secretion was substantially and gradually decreased by peptide glycosylation with carbohydrates of increasing size.

That the improved internalization of [^{123}I]Gluc-TOC, [^{123}I]Gluc-TOCA, [^{123}I]Gluc-*S*-TOCA, and [^{123}I]Gal-*S*-TOCA is indeed induced by an effect of radioligand structure on the internalization of the receptor−ligand complex and not by transport of the glycopeptides via membrane-associated carbohydrate transporters has been verified by a competition experiment. Both in the absence and in the presence of different glucose and/or mannose concentrations in the assay medium, the ratio of the amount of internalized glycosylated radiopeptide to the amount of [^{125}I]TOC (see Figure 3) remained unchanged (data not shown). Absolute cellular uptake as a percentage of the applied activity of both the glycosylated compound of interest and [^{125}I]TOC, however, was increased in the presence of increasing amounts of glucose, indicating the energy dependence of the internalization process.

Ligand internalization of all compounds investigated correlates well with the corresponding EC$_{50,R}$ (Figure 6). The latter value represents a measure of the radioligand's ability to compete with unlabeled TOC for receptor binding and subsequent endocytosis into the cell; the higher this value is, the more unlabeled competitor is necessary to inhibit radioligand internalization and thus the better the radioligand's internalization potency. It is therefore not surprising that the absolute amount of cellular activity uptake should correlate with this quantity. As demonstrated in Figure 6, the EC$_{50,R}$ therefore may represent an accurate predictive value for the ability of a new radioligand to be efficiently internalized into hsst$_2$-expressing cells.

Interestingly, the above correlation was only observed in CHO cells stably transfected with hsst$_2$. In AR42J cells from a rat pancreatic acinar tumor cell line expressing rsst$_2$, the internalization of [^{123}I]Gluc-TOCA compared to [^{125}I]TOC is increased by a factor of 2.8 (CHO cells: 1.9), while the increase in EC$_{50,R}$ is negligible (Figure 4B). Thus, the enhanced internalization

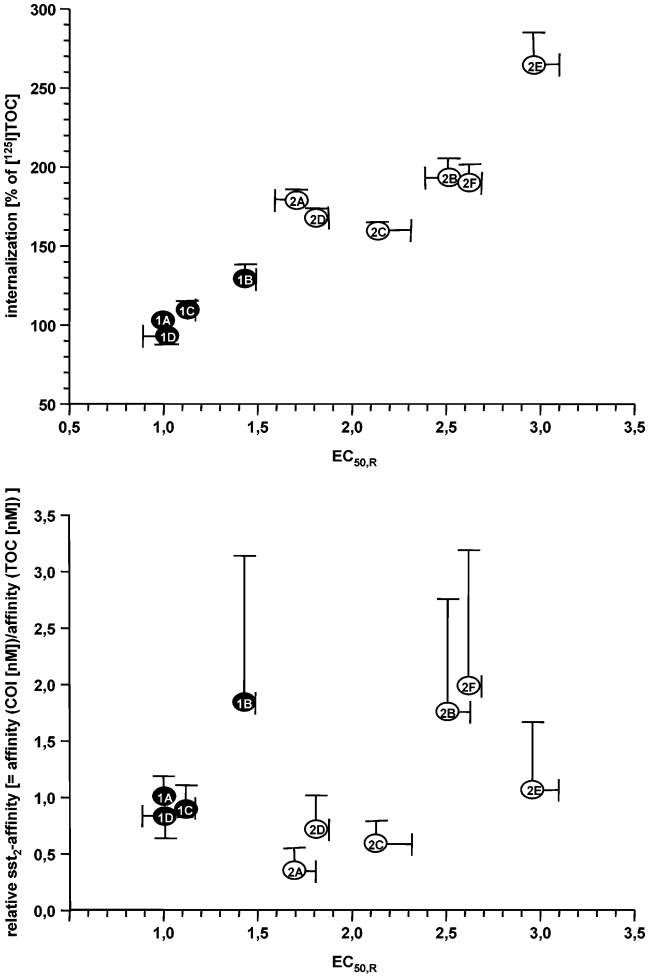

Figure 6. (Top) $EC_{50,R}$ vs internalization (as percent of [^{125}I]TOC) of all compounds investigated (CHO cells, 10 min incubation). (Bottom) $EC_{50,R}$ vs relative $hsst_2$ affinity of all compounds investigated (COI = compound of interest).

of [^{123}I]Gluc-TOCA in AR42J cells does not seem to be the result of more efficient receptor binding of the radioligand compared to [^{125}I]TOC and thus more efficient ligand internalization, which had been observed for [^{123}I]Gluc-TOCA in CHO cells. In contrast, data indicate that in the case of AR42J cells sugar conjugation and C-terminal oxidation lead to a dramatically enhanced internalization *rate* of [^{123}I]Gluc-TOCA. Since [^{123}I]Gluc-TOCA and [^{125}I]TOC bind to the receptor with similar efficiency, as reflected by the $EC_{50,R}$ close to 1 (Figure 4B), the observed drastic increase in internalization of [^{123}I]Gluc-TOCA by a factor greater than 2.5 compared to [^{125}I]TOC can only be explained by an *accelerated* radioligand uptake into the cell. That the rate of receptor internalization and receptor desensitization induced by the same receptor ligand in different cell lines can vary substantially has already been demonstrated for δ-opioid receptors.[51] Results differed significantly between nonneuronal cells transfected with the respective receptor (corresponding to CHO cells transfected with $hsst_2$ used in this study) and cells of neuronal phenotype, which endogenously express δ-opioid receptors at physiological levels (corresponding to AR42J tumor cells that endogenously express $rsst_2$).

That the internalization rate of [^{123}I]Gluc-TOCA is indeed enhanced compared to [^{125}I]TOC in AR42J cells is further supported by data from the comparative externalization experiments in both CHO and AR42J cells (Figure 5). Under conditions allowing recycling, i.e., reinternalization after externalization, both [^{125}I]TOC and [^{123}I]Gluc-TOCA show comparable and low externalization from CHO cells within 60 min. In previous studies it has been demonstrated in detail that the externalization rate of intact radioligand from sst_2-expressing cells is independent of radioligand structure.[24] The same has been observed in this study, independent of the cell line used, when ligand recycling was inhibited by an excess of cold TOC in the external medium (Figure 5). Thus, the amount of [^{125}I]TOC and [^{123}I]Gluc-TOCA being externalized can be assumed to be comparable at all time points. Furthermore, since radioligand concentrations in the external medium are very low under the given experimental conditions, no competition for receptor binding between externalized [^{125}I]TOC and [^{123}I]Gluc-TOCA and hence no effect of an enhanced $EC_{50,R}$ of [^{123}I]Gluc-TOCA vs [^{125}I]TOC can be expected. Thus, the major factor determining the radioligand levels remaining inside the cells is the recycling rate, which in the case of CHO cells is shown to be equally fast for both peptides. When AR42J cells are used, the overall extent of ligand externalization under conditions allowing recycling is enhanced compared to CHO cells, and externalization of [^{123}I]Gluc-TOCA is apparently significantly slower than that of [^{125}I]TOC. On the basis of the argument above, this observation may be explained by faster reinternalization, i.e., a higher internalization rate, of [^{123}I]Gluc-TOCA compared to the nonmodified peptide, which is in accordance with data from the $EC_{50,R}$ and internalization studies.

Other important factors influencing ligand externalization and recycling, however, are intracellular trafficking of the ligand−receptor complex and the extent of ligand degradation. Upon internalization of the ligand−receptor complex, it can be targeted either to endosomes for externalization of both receptor and ligand or to lysosomes for their degradation. Which of the two routes is prefentially taken depends mainly on the nature of the receptor ligand. In the case of δ-opioid receptors it has been demonstrated that upon binding of peptidic receptor ligands, the receptors are mainly targeted toward lysosomal degradation, whereas almost no degradation, but only ligand and receptor reexternalization and recycling, occurred when an alkaloid agonist was used.[52] In the case of the externalization study using CHO cells, the experiment under conditions inhibiting ligand recycling (Figure 5A) showed that more than 94% of the intracellularly accumulated ligand, independent of its structure ([^{123}I]Gluc-TOCA vs [^{125}I]TOC), was externalized within 60 min, indicating an almost exclusive role of receptor and ligand externalization and recycling. In contrast, 35−40% of internalized [^{123}I]Gluc-TOCA and [^{125}I]TOC remain inside the AR42J cells in the corresponding experiment. At first glance, this finding indicates a higher fraction of lysosomal targeting of receptor and radioligand in this cell line compared with CHO cells. The apparent "trapping" of radioactivity in AR42J cells, however, needs further investigation. So far, data (Figure 5) indicate a reduced rate of externalization from AR42J cells. It seems probable that longer observation periods (up to

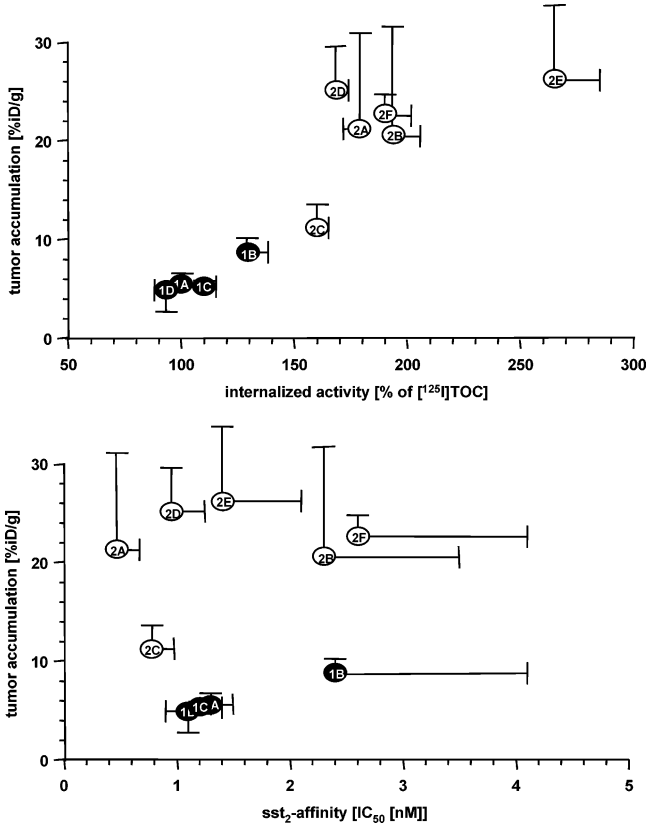

Figure 7. (Top) Internalization (as percent of [^{125}I]TOC, CHO cells, 10 min incubation) of all compounds investigated vs tumor accumulation in AR42J tumor bearing nude mice 60 min p.i. (Bottom) hsst$_2$ affinity (IC_{50} [nM]) of all compounds investigated vs tumor accumulation in AR42J tumor-bearing nude mice 60 min p.i.

240 min) may demonstrate the expected washout of radioiodinated fragments such as [*I]iodotyrosine from the cells.

As demonstrated in Figure 7, in vivo tumor accumulation of [^{125}I]TOC, [^{125}I]TOCA, and their glycosylated analogues in AR42J tumor-bearing nude mice parallels the results obtained in the in vitro studies using CHO cells. While tumor accumulation clearly correlates with the internalization of the respective radiopeptide and thus also is a function of the ligand's $EC_{50,R}$ (see Figure 6), it does not correlate with the hsst$_2$ affinity of the ligand. This finding again illustrates a special feature of some of the radioiodinated carbohydrated somatostatin analogues investigated in this study, i.e., [^{123}I]Gluc-TOC, [^{123}I]Gluc-TOCA, [^{123}I]Gluc-*S*-TOCA, and [^{123}I]Gal-*S*-TOCA: the enhancement of peptide accumulation in receptor expressing cells, in vitro and in vivo, despite reduced receptor affinity compared to their noncarbohydrated analogues.

Conclusion

Both modifications introduced into [^{125}I]TOC, C-terminal Thr-for-Thr(ol) exchange, and N-terminal derivatization with different carbohydrates have significant impact on radioligand uptake into sst$_2$-expressing cells, both in vitro and in vivo. Glucose conjugation via Amadori reaction alone already leads to improved tumor uptake of [^{123}I]Gluc-TOC in vivo, which is based on an enhancement of peptide internalization despite a reduction in receptor affinity. In the case of the doubly modified analogues [^{123}I]Gluc-TOCA, [^{123}I]Gluc-*S*-TOCA and [^{123}I]Gal-*S*-TOCA, a cumulative effect of both structural modifications was observed, leading to up to 5-fold uptake of these compounds in sst-expressing tumors compared to [^{125}I]TOC. Thus, in this study glycosylation with small carbohydrates, especially with the Gluc-*S* moiety, was found to be a suitable tool to enhance receptor-mediated uptake of radiolabeled octreotide analogues into sst-positive malignancies. The availability of different and chemically straightforward glycosylation methods not only allows further "fine-tuning" of ligand characteristics but also makes this approach easily adaptable to a variety of other neuropeptide analogues. Since the limited residualization of radioiodinated receptor ligands in their target cells still hampers their application for therapeutic interventions in nuclear medicine, further efforts are directed toward the combination of the beneficiary effects of C-terminal oxidation and N-terminal glycosylation with labeling methods leading to higher retention of radioactivity in the target cells.

Materials and Methods

1. Peptide Synthesis. 1.1. General Conditions. TCP (trityl chloride polystyrene) resin was obtained from PepChem (Tübingen, Germany). DHP-HM (3,4-dihydro-2*H*-pyran-2-yl-methoxymethylpolystyrene) resin, Fmoc amino acid, and other amino acids were supplied by Novabiochem (Bad Soden, Germany). IodoGen (1,3,4,6-tetrachloro-3α,6α-diphenylglycoluril) came from Pierce (Rockford, IL). All other reagents were purchased from VWR (Darmstadt, Germany), Alexis (Grünberg, Germany), and Aldrich and Fluka (Neu-Ulm, Germany). Solvents were used without further purification.

Solid phase peptide synthesis was carried out manually using a flask shaker (St. John Associates Inc.).

Analytic RP-HPLC was performed on Nucleosil 100 C18 (5 μm, 250 mm × 4 mm or 125 mm × 4.0 mm) columns (CS GmbH, Langerwehe, Germany) using a Sykam gradient HPLC system (Sykam, Fürstenfeldbruck, Germany). The peptides were eluted applying various gradients of 0.1% TFA in H_2O (solvent A) and 0.1% TFA in acetonitrile (solvent B) in 30 and 15 min, respectively, at a constant flow of 1 mL/min. UV detection was performed at 220 nm in a 206 PHD UV−vis detector (Linear Instruments Corporation, Reno, NV). For radioactivity measurement, the outlet of the UV photometer was connected to a NaI(Tl) well-type scintillation counter from EG&G Ortec (München, Germany).

Preparative RP-HPLC was performed on the same HPLC system using a Multospher 100 RP 18-5 (250 mm × 10 mm) column (CS GmbH, Langerwehe, Germany) at a constant flow of 5 mL/min.

ESI mass spectra were recorded on an LCQ LC−MS system from Finnigan (Bremen, Germany) using the Hewlett-Packard series 1100 HPLC system.

1.2. Precursors for Radioiodination. 1.2.1. Tyr^3-Lys^5-(Dde)-octreotide (TOC(Dde)). The synthesis of TOC(Dde) was performed as described previously for TOC.[39] Briefly, freshly prepared Fmoc-Thr(tBu)-ol[39,53] was anchored to DHP-HM resin in the presence of pyridinium *p*-toluenesulfonate at 80 °C in dry 1,2-dichloroethane. Assembly of the peptide sequence H_2N-dPhe-Cys(Trt)-Tyr-dTrp-Lys(Dde)-Thr-Cys(Trt) on the resin-bound amino alcohol was performed according to standard Fmoc protocol using 1.5 equiv of HOBt (1-hydroxybenzotriazole) and TBTU (*O*-(1*H*-benzotriazol-1-yl)-*N*,*N*,*N*′,*N*′-tetramethyluronium tetrafluoroborate) as coupling reagents and *N*-ethyldiisopropylamine (DIEA) as a base. The peptide was cleaved from the resin using a 1:1 mixture (v/v) of (95% TFA, 2.5% TIBS (triisobutylsilane), 2.5% H_2O (v/v/v)) and DCM (dichloromethane). Disulfide bridge formation was achieved using H_2O_2 in a THF (tetrahydrofurane)/5 mM NH_4OAc mixture buffered to pH 7 with saturated $NaHCO_3$. TOC(Dde)

was obtained in 86% yield based on the resin-bound amino alcohol. HPLC (30% → 80% in 15 min): t_R(cyclic peptide) = 8.0 min; K' = 4.30. Calculated monoisotopic mass for of TOC(Dde) ($C_{59}H_{78}N_{10}O_{13}S_2$) = 1198.5. Found: m/z = 1199.3 $[M + H]^+$, m/z = 1221.3 $[M + Na]^+$

1.2.2. Tyr³-Lys⁵(Dde)-octreotate (TOCA(Dde)). Fmoc-Thr(tBu)-OH (596 mg, 1.5 mmol) was dissolved in 15 mL of dry DCM, and an amount of 214 μL of DIEA (1.25 mmol) was added. Dry TCP resin (1.0 g, 1.0 mmol of trityl chloride groups) was suspended in this solution and stirred at room temperature for 5 min. Another quantity of 428 μL of DIEA (2.5 mmol) was added, and stirring was continued for 90 min. Then 1 mL of MeOH (methanol) was added to cap unreacted trityl chloride groups. After 15 min the resin was filtered off, washed twice with DCM, DMF (*N*,*N*-dimethylformamide), and MeOH, and dried in vacuo. The final load of resin-bound Fmoc-Thr(tBu)-OH was calculated to be 0.74 mmol/g using the following formula:

$$\text{load [mmol/g]} = \frac{1000(m_2 - m_1)}{(\text{MW} - 36.461\ \text{g/mol})m_2}$$

m_1 = mass of the dry TPC resin before coupling [g]

m_2 = mass of the dried resin after the coupling reaction [g]

MW = molecular weight of the Fmoc-amino acid [g/mol]

After SPPS (see TOC(Dde)), the peptide was cleaved from the solid support using 95% TFA, 2.5% TIBS, and 2.5% H_2O (v/v/v). Cyclization of the crude peptide was performed in analogy to TOC(Dde). Yield based on resin-bound Thr: 97%. HPLC (30% → 80% in 15 min): t_R(cyclic peptide) = 8.4 min; K' = 4.45. Calculated monoisotopic mass for of TOCA(Dde) ($C_{59}H_{76}N_{10}O_{14}S_2$) = 1212.5. Found: m/z = 1213.6 $[M + H]^+$, m/z = 1235.7 $[M + Na]^+$.

1.2.3. Peptide Glycosylation via Amadori Reaction. On the basis of a previously reported method,[50] 1 equiv of Lys⁵(Dde)-protected peptide and 10 equiv of the respective aldose (glucose, maltose, maltotriose) were dissolved in 1 mL of MeOH (5% AcOH (acetic acid)) per 100 mg of peptide, and the reaction mixture was stirred at 60 °C for 16−48 h. The crude products were precipitated using Et_2O (diethyl ether) and dried in vacuo.

1.2.4. Dde Deprotection. To a solution of 50−200 mg of peptide in 980 μL of DMF, an amount of 20 μL of hydrazine hydrate was added. After 10 min at room temperature, the deprotected product was precipitated using Et_2O, washed with Et_2O, and dried in vacuo. All deprotected peptides were subsequently purified using preparative gradient HPLC.

1.2.5. N_α-(1-*S*-(α-D-Glucopyranosyl)-3-mercaptopropionyl)-D-Phe¹-Tyr³-octreotate and N_α-(1-*S*-(α-D-Galactopyranosyl)-3-mercaptopropionyl)-D-Phe¹-Tyr³-octreotate (Gluc-*S*-TOCA and Gal-*S*-TOCA). 1-*S*-(2,3,4,6-Tetraacetylglucopyranosyl)-3-mercaptopropionate and 1-*S*-(2,3,4,6-Tetraacetylgalactopyranosyl)-3-mercaptopropionate.[54] To a solution of peracetylated sugar (3 mmol, 1.17 g) and mercaptopropionic acid (12 mmol, 1.04 mL) in 20 mL of dry dichloromethane, $BF_3{\cdot}Et_2O$ (4.5 mmol, 565 μL) was slowly added. Product formation was monitored via TLC (AcOEt/hexane/AcOH: 10/10/1 (v/v/v)). The solution was stirred at room temperature for 4 h, diluted with dichloromethane, and extracted with 1 M HCl. The aqueous phase was then extracted once with dichloromethane. The combined organic phases were dried over $MgSO_4$, filtered, and evaporated to dryness. After purification via column chromatography (AcOEt/hexane/AcOH: 10/10/1 (v/v/v)), 1.01 g (77%) of 2,3,4,6-tetraacetyl-1-*S*-mercaptopropionylglucose were obtained as a white solid, whereas 2,3,4,6-tetraacetyl-1-*S*-mercaptopropionylgalactose was obtained as a clear oil in 88% yield.

1-*S*-(2,3,4,6-Tetraacetylglucopyranosyl)-3-mercaptopropionic Acid Pentafluorophenyl Ester and 1-*S*-(2,3,4,6-Tetraacetylgalactopyranosyl)-3-mercaptopropionic Acid Pentafluorophenyl Ester (Gluc(4Ac)-*S*-OPfp and Gal(4Ac)-*S*-OPfp). The respective 1-*S*-(2,3,4,6-tetraacetylglycosyl)-3-mercaptopropionate (1 equiv) was dissolved in 30 mL of THF, and *N*,*N*′-diisopropylcarbodiimide (1.1 equiv), followed by pentafluorophenol (1.1 equiv) in 3 mL of THF, was added. After 24 h, reaction control via TLC (AcOEt/hexane: 4/6 (v/v)) revealed complete disappearance of the starting material. The solvent was evaporated, and the crude product was purified using column chromatography (AcOEt/hexane: 4/6), yielding the respective pentafluorophenyl active esters in 80−89% yield (Gluc-*S*-OPfp, white solid; Gal-*S*-OPfp, clear oil). ^{1}H NMR Gluc-*S*-OPfp ($CDCl_3$, 250 MHz): δ (ppm) 2.04, 2.06, 2.09, 2.11 (4 s, each 3 H, 4 Ac), 3.03−3.14 (m, 4 H, SCH_2CH_2COOH), 3.74−3.81 (m, 1 H, H-5), 4.15−4.31 (m, 2H, H-6), 4.6 (d, 1 H, J = 10 Hz, H-1), 5.09 (t, 1 H, J = 10, 9.25 Hz, H-2), 5.13 (t, 1 H, J = 10, 9.25 Hz, H-4), 5.25 (d, 1 H, J = 9.5 Hz, H-3).

Gluc-*S*-TOCA and Gal-*S*-TOCA. TOCA(Dde) (50−100 mg, 1 equiv) and Gluc/Gal(4Ac)-*S*-OPfp (1.1 equiv) were dissolved in 1−2 mL of DMF and stirred at room temperature for 2 h in the presence of 1 equiv of DIEA. After product precipitation using Et_2O and washing of the precipitate with Et_2O, the respective glycosylated peptides were obtained in 46−67% yield. (Gluc(4Ac)-*S*-TOCA(Dde): HPLC (30 → 80% B in 15 min) t_R = 12.1 min; K' = 6.31. Gal(4Ac)-*S*-TOCA(Dde): HPLC (30 → 80% B in 15 min) t_R = 12.0 min; K' = 6.42)

After Dde deprotection for 10 min at room temperature, the peptides were precipitated using Et_2O. For subsequent sugar deacetylation, peptides were redissolved in 1 mL of MeOH containing 0.5 equiv of KCN. Deacetylation was complete after stirring at room temperature for 4−48 h. The product was then precipitated using Et_2O and purified via preparative HPLC, yielding Gluc-*S*-TOCA and Gal-*S*-TOCA in yields of 12−15% (based on TOCA(Dde)).

Synthetic data for all radioiodination precursors are summarized in Table 4.

1.3. 3-Iodo-Tyr³ Reference Compounds. For the synthesis of the 3-iodo-Tyr³ reference compounds, Fmoc-Tyr(tBu)-OH was replaced by Fmoc-3-iodo-Tyr(tBu)-OH during SPPS of TOC(Dde) and TOCA(Dde). All other reaction steps were performed analogously to the syntheses presented in the previous section. Yields for all glycosylated peptides after preparative HPLC (based on the respective nonglycosylated Dde-protected precursors) were 18−24%.

Synthetic data for all 3-iodo-Tyr³ reference compounds are summarized in Table 4.

2. Peptide Radioiodination. Radioiodination was generally performed using the Iodogen method.

A solution of 100−200 μg of peptide in 200 μL of PBS (phosphate buffered saline, 0.1M, pH 7.4) was transferred to an Eppendorf tube coated with 30 μg of Iodogen (Pierce, Rockford, IL). After the addition of 5−20 μL of solution of radioiodide (Amersham, Buckinghamshire, U.K.) in 0.05 M NaOH ($[^{125}I]$NaI (n.c.a.), 18−74 MBq; $[^{123}I]$NaI (c.a.), 37−185 MBq), the cap was vortexed and the labeling reaction was allowed to proceed for 20 min at room temperature. The peptide solution was then removed from the insoluble oxidizing agent.

The radioiodinated peptides were purified via RP-HPLC (Nucleosil 100 C18 column (5 μm, 125 mm × 4.0 mm) at a constant flow of 1 mL/min using an isocratic solvent mixture of 25% $[^{123}I]$Mtr-TOCA, 26% $[^{123}I]$Gluc-TOC, 27% $[^{123}I]$Malt-TOC, $[^{123}I]$Mtr-TOC, and $[^{123}I]$Malt-TOCA, 28% $[^{125}I]$TOC, $[^{123}I]$TOCA, and $[^{123}I]$Gluc-TOCA, or 33% $[^{123}I]$Gluc-*S*-TOCA and $[^{123}I]$Gal-*S*-TOCA, and EtOH (0.5% AcOH) in water (0.5% AcOH). Radiochemical yields after purification ranged from 45% to 85%. HPLC data for all radioiodinated peptides and the solvent composition applied for quality control HPLC are given in Table 5.

For the biodistribution experiments, an excess of absolute ethanol was added to the collected fraction, and the solvents were evaporated to dryness. The radioiodinated product was redissolved in PBS to yield a solution of radiolabeled peptide with an activity concentration of approximately 370 kBq/100 μL.

For the paired-label internalization experiments, $[^{125}I]$TOC and the respective ^{123}I-labeled radioligand were each redis-

Table 4. Synthetic Data of All Radioiodination Precursors and Their Corresponding 3-Iodo-Tyr^3 Analogues

peptide		HPLC characterization: gradient	t_R [min]	K'	sum formula	ESI mass spectrometry characterization: calcd MW [g/mol]	m/z $[M + H]^+$	m/z $[M + Na]^+$
TOC		10% → 60% B (30 min)	12.9	4.48	$C_{49}H_{66}N_{10}O_{11}S_2$	1034.4	1035.2	1057.3
Gluc[a]-TOC		10% → 60% B (30 min)	13.1	4.13	$C_{55}H_{76}N_{10}O_{16}S_2$	1196.5	1197.2	1219.3
Malt[b]-TOC		10% → 60% B (30 min)	12.6	3.85	$C_{61}H_{86}N_{10}O_{21}S_2$	1358.5	1359.2	1381.3
Mtr[c]-TOC		10% → 60% B (30 min)	13.1	3.78	$C_{67}H_{96}N_{10}O_{26}S_2$	1520.6	1521.2	1543.3
TOCA		10% → 60% B (30 min)	16.3	5.54	$C_{49}H_{64}N_{10}O_{12}S_2$	1048.4	1049.1	1071.2
Gluc-TOCA		10% → 60% B (30 min)	15.4	4.68	$C_{55}H_{74}N_{10}O_{17}S_2$	1210.5	1211.5	1233.5
Malt-TOCA		10% → 60% B (30 min)	14.8	4.59	$C_{61}H_{84}N_{10}O_{22}S_2$	1372.5	1373.1	1395.6
Mtr-TOCA		10% → 60% B (30 min)	14.5	4.48	$C_{67}H_{94}N_{10}O_{27}S_2$	1534.6	1535.2	1557.2
Gluc-*S*-TOCA		20% → 70% B (15 min)	8.2	3.99	$C_{58}H_{78}N_{10}O_{18}S_3$	1298.5	1299.3	1321.3
Gal-*S*-TOCA		20% → 70% B (15 min)	8.3	3.96	$C_{58}H_{78}N_{10}O_{18}S_3$	1298.5	1299.3	1321.3
I-TOC	**1A**	10% → 60% B (30 min)	16.3	5.79	$C_{49}H_{65}N_{10}O_{11}S_2I$	1160.3	1161.1	1183.1
I-Gluc-TOC	**1B**	10% → 60% B (30 min)	15.8	5.58	$C_{55}H_{75}N_{10}O_{16}S_2I$	1322.4	1323.1	1345.2
I-Malt-TOC	**1C**	10% → 60% B (30 min)	15.7	5.54	$C_{61}H_{85}N_{10}O_{21}S_2I$	1484.4	1485.2	
I-Mtr-TOC	**1D**	10% → 60% B (30 min)	15.2	5.33	$C_{67}H_{95}N_{10}O_{26}S_2I$	1646.5	1647.1	1669.3
I-TOCA	**2A**	10% → 60% B (30 min)	17.0	5.08	$C_{49}H_{63}N_{10}O_{12}S_2I$	1174.3	1175.0	
I-Gluc-TOCA	**2B**	10% → 60% B (15 min)	11.1	5.17	$C_{55}H_{73}N_{10}O_{17}S_2I$	1336.4	1337.0	1359.3
I-Malt-TOCA	**2C**	10% → 60% B (30 min)	16.1	5.69	$C_{61}H_{85}N_{10}O_{21}S_2I$	1498.4	1499.2	
I-Mtr-TOCA	**2D**	10% → 60% B (15 min)	11.2	6.33	$C_{67}H_{93}N_{10}O_{27}S_2I$	1660.5	1661.2	1683.2
I-Gluc-*S*-TOCA	**2E**	20% → 70% B (15 min)	9.2	4.72	$C_{58}H_{77}N_{10}O_{18}S_3I$	1424.4	1425.6	1447.6
I−Gal-*S*-TOCA	**2F**	20% → 70% B (15 min)	9.1	4.79	$C_{58}H_{77}N_{10}O_{18}S_3I$	1424.4	1425.6	1447.6

[a] N_α-(1-Deoxy-D-fructosyl). [b] N_α-(α-D-Glucopyranosyl-(1−4)-1-deoxy-D-fructosyl). [c] N_α-(*O*-α-D-Glucopyranosyl-(1−4)-*O*-α-D-glucopyranosyl)-(1−4)-1-deoxy-D-fructosyl).

Table 5. HPLC Data for All Radioiodinated Peptides

	% EtOH in isocratic eluent	t_R [min]	K'
[^{125}I]TOC	29	9.5	5.52
[^{123}I]Gluc-TOC	27	10.2	8.14
[^{123}I]Malt-TOC	27	7.2	5.70
[^{123}I]Mtr-TOC*	27	8.1	6.71
[^{123}I]TOCA	28	10.2	10.10
[^{123}I]Gluc-TOCA	29	8.0	7.80
[^{123}I]Malt-TOCA	27	10.1	7.78
[^{123}I]Mtr-TOCA	25	7.5	7.30
[^{123}I]Gluc-*S*-TOCA	32	8.7	9.36
[^{123}I]Gal-*S*-TOCA	33	7.5	7.95

solved in assay medium (containing 5% BSA) and diluted to an activity concentration of approximately 200 000 cpm/10 μL. A 1:1 (v/v) mixture of both solutions containing approximately 100 000 cpm/10 μL of each radioligand was then used for the internalization experiment.

3. Cell Culture. AR42J cells were obtained from ECACC (European Collection of Cell Cultures, Salisbury, U.K.). Cells were maintained in RPMI 1640 (Seromed, Berlin, Germany) supplemented with 10% FCS (Seromed) and 2 mM L-glutamine (Gibco BRL Life Technologies, Karlsruhe, Germany). CHO cells stably transfected with human sst_2 (epitope tagged at the N-terminal end) were kindly provided by Dr. Jenny Koenig, University of Cambridge, U.K. Cells were grown in DMEM/nutrition mix F-12 with Glutamax-I (1:1) (Gibco BRL) supplemented with 10% FCS and 500 mg/L Geneticin (Gibco BRL). Cultures were maintained at 37 °C in a 5% CO_2/humidified air atmosphere.

In the assay medium used for internalization studies, FCS was replaced by 1% BSA (Sigma, St. Louis, MO).

For cell counting, a CASY1-TT cell counter and analyzer system (Schärfe System GmbH, Reutlingen, Germany) was used.

4. In Vitro Studies. 4.1. sst-Receptor Binding Affinities and Subtype Specificities (CHO-K1 and CCL39 Cells). Cells stably expressing human sst_1, sst_2, sst_3, sst_4, and sst_5 (sst_1 and sst_5, CHO-K1 cells; sst_{2-4}, CCL39 cells) were grown as described previously.[48] Cell membrane pellets were prepared, and receptor autoradiography was performed on pellet sections (mounted on microscope slides), as described in detail previously.[48] For each of the tested I-TOC and I-TOCA derivatives, complete displacement experiments were performed with the universal somatostatin radioligand [^{125}I]-[Leu^8,D-Trp^{22},Tyr^{25}]somatostatin 28 [48] using increasing concentrations of the unlabeled peptide ranging from 0.1 to 1000 nM. Somatostatin 28 was run in parallel as control using the same increasing concentrations. IC_{50} values were calculated using a computer-assisted image-processing system. Tissue standards (autoradiographic [^{125}I]microscales Amersham), containing known amounts of isotopes and cross-calibrated to tissue equivalent ligand concentrations, were used for quantification.[48]

4.2. Internalization and Determination of $EC_{50,R}$ (CHO and AR42J). One day prior to the experiment, cells were harvested using Trypsin/EDTA (0.05% and 0.02%) in PBS, centrifuged, and resuspended with culture medium. Concentration of the suspension ranged from 40 000 to 60 000 cells/mL in the case of CHO cells and from 180 000 to 250 000 cells/mL in the case of AR42J cells. The suspension was transferred into 24-well plates (1 mL/well) and placed in the incubator overnight.

On the day of the experiment (cell count for CHO, 90000−120000 cells/well; cell count for AR42J, 200000−250000 cells/well), the culture medium was removed and the cells were washed once with 250 μL of medium (unsupplemented DMEM (CHO cells) or RPMI-1640 (AR42J cells)) before being left to equilibrate in 190 μL of medium at 37 °C for a minimum of 15 min before the experiment. Then 50 μL (per well) of medium (5% BSA) containing increasing concentrations of unlabeled TOC were added, followed by the addition of approximately 100 000 cpm of both the respective ^{123}I-labeled peptide and of the reference [^{125}I]TOC in 10 μL of medium (5% BSA). Final TOC concentrations in the incubation medium were 0.1, 0.2, 0.5, 0.8, 1, 2, 4, 6, 8, 10, 12, 15, 20, 50, 100, 500, and 1000 nM. In a control experiment (n.c.a. conditions), ligand-free medium (5% BSA) was added. Nonspecific internalization was determined by including 5 μM unlabeled TOC. Experiments were carried out in triplicate for each concentration.

After the addition of the radioligands, the cells were incubated for 10 min (CHO) or 30 min (AR42J) at 37 °C. To ensure a constant incubation temperature, the plates were placed into a sand bath inside the incubator.

Incubation was terminated by placing the plate on an ice pack for approximately 1 min and by subsequent removal of the incubation medium. Cells were thoroughly rinsed with 250 μL of fresh medium. The wash medium was combined with the supernatant of the previous step. This fraction represents the amount of free radioligand. To remove surface-bound (acid releasable) radioactivity, the cells were then incubated with 250 μL of ice-cold acid wash buffer (0.02 M NaOAc buffered with AcOH to pH 5). After removal of the acid wash buffer, the cells were thoroughly rinsed with another 250 μL of ice-

cold acid wash buffer. Both acid wash fractions were combined. The internalized activity was released by incubation with 250 μL of 1 N NaOH, tranferred to vials, and combined with 250 μL of PBS used for rinsing the wells. Quantification of the amount of free, acid-releasable, and internalized activity was performed in a γ-counter.

For numerical analysis of the EC_{50} of TOC for internalization, data for both the ^{123}I-labeled compound of interest and for the reference [^{125}I]TOC in the same experiment were first corrected by the amount of nonspecific internalization, respectively, and then each was normalized to the amount of internalized ligand in the absence of unlabeled competitor (100%). Data were fitted with a weighted two-parameter logistic function using SigmaPlot. To eliminate the influence of cell count and cell viability on the absolute EC_{50} values, data are expressed as the ratio ($EC_{50,R}$) of the EC_{50} observed for the compound of interest (COI) to the EC_{50} found for [^{125}I]TOC in the same experiment ($EC_{50,R} = EC_{50}(COI)/EC_{50}([^{125}I]TOC)$).

4.3. Externalization and Recycling (CHO and AR42J). As in the previous experiment, cells were incubated with the respective ^{123}I-labeled peptide and the reference [^{125}I]TOC at 37 °C for 10 (30) min and washed with medium. To ensure receptor integrity, no acid wash was performed after this initial internalization incubation. Then, to determine the extent of ligand recycling, two different experiments were performed. In the experiment allowing ligand recycling, 200 μL of medium and 50 μL of medium (5% BSA) were added to each well. In the experiment inhibiting ligand recycling, 200 μL of assay medium and 50 μL of medium (5% BSA) containing 25 μM TOC were added to each well. Experiments were carried out in triplicate for both experimental conditions. Subsequently, the cells were incubated at 37 °C for 30 and 60 min. The supernatant was removed and combined with 250 μL of medium used for rinsing the cells. This fraction represents the amount of externalized ligand. The subsequent steps, i.e., acid wash and lysis of the cells, were performed as described for the internalization experiment.

5. In Vivo Biodistribution Studies. 5.1. Animal Model. For all in vivo experiments, nude mice (Swiss nu/nu, female, 6−8 weeks) were used. To establish tumor growth, AR42J cells were treated with 1 mM EDTA in PBS, suspended, centrifuged, and resuspended in serum-free RPMI 1640. Mice were inoculated subcutaneously in the flank with $(2.5-5) \times 10^6$ cells. Ten days after inoculation, all mice showed solid palpable tumor masses (tumor weight of 150−500 mg) and were used for the experiments.

5.2. Biodistribution Studies. About 370 kBq (10 μCi) of the ^{125}I-labeled peptides in 100 μL of PBS (pH 7.4) were injected intravenously (iv) into the tail vein of nude mice bearing an AR42J tumor. The animals were sacrificed 60 min postinjection (p.i.) ($n = 5$), and the organs of interest were isolated. The radioactivity was measured in weighed tissue samples using a γ-counter. Data are expressed as % ID/g tissue (mean ± SD).

References

(1) Reubi, J. C.; Krenning, E.; Lamberts, S. W.; Kvols, L. Somatostatin receptors in malignant tissues. *J. Steroid Biochem. Mol. Biol.* **1990**, *37* (6), 1073−1077.

(2) Reubi, J. C.; Laderach, U.; Waser, B.; Gebbers, J. O.; Robberecht, P.; Laissue, J. A. Vasoactive intestinal peptide/pituitary adenylate cyclase-activating peptide receptor subtypes in human tumors and their tissues of origin. *Cancer Res*. **2000**, *60* (11), 3105−3112.

(3) Reubi, J. C. In vitro evaluation of VIP/PACAP receptors in healthy and diseased human tissues. Clinical implications. *Ann. N.Y. Acad. Sci*. **2000**, *921*, 1−25.

(4) Reubi, J. C.; Gugger, M.; Waser, B. Co-expressed peptide receptors in breast cancer as a molecular basis for in vivo multireceptor tumour targeting. *Eur. J. Nucl. Med. Mol. Imaging* **2002**, *29* (7), 855−862.

(5) Reubi, J. C.; Waser, B.; Schaer, J. C.; Laissue, J. A. Neurotensin receptors in human neoplasms: high incidence in Ewing's sarcomas. *Int. J. Cancer* **1999**, *82* (2), 213−218.

(6) Reubi, J. C.; Zimmermann, A.; Jonas, S.; Waser, B.; Neuhaus, P.; Laderach, U.; Wiedenmann, B. Regulatory peptide receptors in human hepatocellular carcinomas. *Gut* **1999**, *45*, 766−774.

(7) Reubi, J. C.; Wenger, S.; Schmuckli-Maurer, J.; Schaer, J. C.; Gugger, M. Bombesin receptor subtypes in human cancers: detection with the universal radioligand ^{125}I-[D-TYR6,beta-ALA11,PHE13,NLE14]bombesin(6−14). *Clin. Cancer Res.* **2002**, *8* (4), 1139−1146.

(8) Reubi, J. C.; Schaer, J. C.; Waser, B. Cholecystokinin (CCK)-A and CCK-B/gastrin receptors in human tumors. *Cancer Res.* **1997**, *57* (7), 1377−1386.

(9) Cassoni, P.; Sapino, A.; Stella, A.; Fortunati, N.; Bussolati, G. Presence and significance of oxytocin receptors in human neuroblastomas and glial tumors. *Int. J. Cancer* **1998**, *77* (5), 695−700.

(10) Bussolati, G.; Cassoni, P.; Ghisolfi, G.; Negro, F.; Sapino, A. Immunolocalization and gene expression of oxytocin receptors in carcinomas and non-neoplastic tissues of the breast. *Am. J. Pathol.* **1996**, *148* (6),1895−1903.

(11) North, W. G. Gene regulation of vasopressin and vasopressin receptors in cancer. *Exp. Physiol.* **2000**, *85*, 27S−40S.

(12) Reubi, J. C. Regulatory peptide receptors as molecular targets for cancer diagnosis and therapy. *Q. J. Nucl. Med.* **1997**, *41*, 63−70.

(13) Bruns, C.; Stolz, B.; Albert, R.; Marbach, P.; Pless, J. OctreoScan 111 for imaging of a somatostatin receptor-positive islet cell tumor in rat. *Horm. Metab. Res., Suppl.* **1993**, *27*, 5−11

(14) Krenning, E. P.; Kwekkeboom, D. J.; Bakker, W. H.; Breeman, W. A.; Kooij, P. P.; Oei, H. Y.; van Hagen, M.; Postema, P. T.; de Jong, M.; Reubi, J. C.; Visser, T. J.; Reijs, A. E. M.; Hofland, L. J.; Koper, J. W.; Lamberts, S. W. J. Somatostatin receptor scintigraphy with [111In-DTPA-D-Phe1]- and [123I-Tyr3]-octreotide: the Rotterdam experience with more than 1000 patients. *Eur. J. Nucl. Med.* **1993**, *20* (8), 716−731.

(15) Otte, A.; Jermann, E.; Béhé, M.; Goetze, M.; Bucher, H. C.; Roser, H. W.; Heppeler, A.; Mueller-Brand, J.; Mäcke, H. R. DOTATOC: a powerful new tool for receptor-mediated radionuclide therapy. *Eur. J. Nucl. Med.* **1997**, *24* (7), 792−795.

(16) Otte, A.; Herrmann, R.; Heppeler, A.; Béhé, M.; Jermann, E.; Powell, P.; Maecke, H. R.; Muller, J. Yttrium-90 DOTATOC: first clinical results. *Eur. J. Nucl. Med.* **1999**, *26* (11), 1439−1447.

(17) Waldherr, C.; Pless, M.; Maecke, H. R.; Schumacher, T.; Crazzolara, A.; Nitzsche, E. U.; Haldemann, A.; Mueller-Brand, J. Tumor response and clinical benefit in neuroendocrine tumors after 7.4 GBq (90)Y-DOTATOC. *J. Nucl. Med.* **2002**, *43*, 610−616.

(18) Virgolini, I.; Raderer, M.; Kurtaran, A.; Angelberger, P.; Banyai, S.; Yang, Q.; Li, S.; Banyai, M.; Pidlich, J.; Niederle, B.; Scheithauer, W.; Valent, P. Vasoactive intestinal peptide-receptor imaging for the localization of intestinal adenocarcinomas and endocrine tumors. *N. Engl. J. Med.* **1994**, *331* (17), 1116−1121

(19) Garcia-Garayoa, E.; Bläuenstein, P.; Bruehlmeier, M.; Blanc, A.; Iterbeke, K.; Conrath, P.; Tourwé, D.; Schubiger, P. A. Preclinical evaluation of a new, stabilized neurotensin(8−13) pseudopeptide radiolabeled with ^{99m}Tc. *J. Nucl. Med.* **2002**, *43*, 374−383.

(20) Behr, T. M.; Jenner, N.; Béhé, M.; Angerstein, C.; Gratz, S.; Raue, F.; Becker, W. Radiolabeled peptides for targeting cholecystokinin-B/gastrin receptor-expressing tumors. *J. Nucl. Med.* **1999**, *40* (6), 1029−1044.

(21) de Jong, M.; Bakker, W. H.; Bernard, B. F.; Valkema, R.; Kwekkeboom, D. J.; Reubi, J. C.; Srinivasan, A.; Schmidt, M.; Krenning, E. P. Preclinical and initial clinical evaluation of ^{111}In-labeled nonsulfated CCK8 analog: a peptide for CCK-B receptor-targeted scintigraphy and radionuclide therapy. *J. Nucl. Med.* **1999**, *40* (12), 2081−2087.

(22) Breeman, W. A.; De Jong, M.; Bernard, B. F.; Kwekkeboom, D. J.; Srinivasan, A.; van der Pluijm, M. E.; Hofland, L. J.; Visser, T. J.; Krenning, E. P. Pre-clinical evaluation of [^{111}In-DTPA-Pro1-Tyr4]bombesin, a new radioligand for bombesin-receptor scintigraphy. *Int. J. Cancer* **1999**, *83* (5), 657−663.

(23) La Bella, R.; Garcia-Garayoa, E.; Langer, M.; Bläuenstein, P.; Beck-Sickinger, A. G.; Schubiger, P. A. In vitro and in vivo evaluation of a ^{99m}Tc(I)-labeled bombesin analogue for imaging of gastrin releasing peptide receptor-positive tumors. *Nucl. Med. Biol.* **2002**, *29*, 553−560.

(24) Koenig, J. A.; Kaur, R.; Dodgeon, I.; Edwardson, J. M.; Humphrey, P. P. Fates of endocytosed somatostatin sst_2 receptors and associated agonists. *Biochem. J.* **1998**, *336*, 291−298.

(25) Csaba, Z.; Bernard, V.; Helboe, L.; Bluet-Pajot, M. T.; Bloch, B.; Epelbaum, J.; Dournaud, P. In vivo internalization of the somatostatin sst2A receptor in rat brain: evidence for translocation of cell-surface receptors into the endosomal recycling pathway. *Mol. Cell. Neurosci.* **2001**, *17*, 646−661.

(26) Hukovic, N.; Panetta, R.; Kumar, U.; Patel, Y. C. Agonist-dependent regulation of cloned human somatostatin receptor types 1−5 (hSSTR1−5): Subtype selective internalization or upregulation. *Endocrinology* **1996**, *137*, 4046−4049.

(27) Froidevaux, S.; Hintermann, E.; Török, M.; Mäcke, H. R.; Beglinger, C.; Eberle, A. N. Differential regulation of somatostatin receptor type 2 (sst 2) expression in AR4-2J tumor cells implanted into mice during octreotide treatment. *Cancer Res.* **1999**, *59*, 3652−3657.
(28) Hofland, L. J.; van Koetsveld, P. M.; Waaijers, M.; Zuyderwijk, J.; Breeman, W. A.; Lamberts, S. W. Internalization of the radioiodinated somatostatin analog [^{125}I-Tyr3]octreotide by mouse and human pituitary tumor cells: Increase by unlabeled octreotide. *Endocrinology* **1995**, *136*, 3698−3706.
(29) de Jong, M.; Breeman, W. A.; Bakker, W. H.; Kooij, P. P.; Bernard, B. F.; Hofland, L. J.; Visser, T. J., Srinivasan, A.; Schmidt, M. A.; Erion, J. L.; Bugaj, J. E.; Mäcke, H. R.; Krenning, E. P. Comparison of ^{111}In-labeled somatostatin analogues for tumor scintigraphy and radionuclide therapy. *Cancer Res.* **1998**, *58*, 437−441.
(30) Lewis, J. S.; Lewis, M. R.; Srinivasan, A.; Schmidt, M. A.; Wang, J.; Anderson, C. J. Comparison of four ^{64}Cu-labeled somatostatin analogues in vitro and in a tumor-bearing rat model: Evaluation of new derivatives for positron emission tomography imaging and targeted radiotherapy. *J. Med. Chem.* **1999**, *42*, 1341−1347.
(31) Bugaj, J. E.; Erion, J. L.; Johnson, M. A.; Schmidt, M. A.; Srinivasan, A. Radiotherapeutic efficiency of ^{153}Sm-CMDTPA-Tyr3-octreotate in tumor-bearing rats. *Nucl. Med. Biol.* **2001**, *28*, 327−334.
(32) Kwekkeboom, D. J.; Bakker, W. H.; Kooij, P. P.; Konijnenberg, M. W.; Srinivasan, A.; Erion, J. L.; Schmidt, M. A.; Bugaj, J. L.; de Jong, M.; Krenning, E. P. [^{177}Lu-DOTA^0,Tyr^3]octreotate: comparison with [^{111}In-DTPA^0]octreotide in patients. *Eur. J. Nucl. Med.* **2001**, *28*, 1319−1325.
(33) De Jong, M.; Valkema, R.; Jamar, F.; Kvols, L. K.; Kwekkeboom, D. J.; Breeman, W. A.; Bakker, W. H.; Smith, C.; Pauwels, S.; Krenning, E. P. Somatostatin receptor-targeted radionuclide therapy of tumors: preclinical and clinical findings. *Semin. Nucl. Med.* **2002**, *32*, 133−140.
(34) Valkema, R.; de Jong, M.; Bakker, W. H.; Breeman, W. A.; Kooij, P. P.; Lugtenburg, P. J.; de Jong, F. H.; Christiansen, A.; Kam, B. L.; de Herder, W. W.; Stridsberg, M.; Lindemans, J.; Ensing, G.; Krenning, E. P. Phase I study of peptide receptor radionuclide therapy with [In-DTPA]octreotide: the Rotterdam experience. *Semin. Nucl. Med.* **2002**, *32*, 110−122.
(35) Janson, E. T.; Westlin, J. E.; Öhrvall, U.; Öberg, K.; Lukinius, A. Nuclear localization of ^{111}In after intravenous injection of [^{111}In-DTPA-D-Phe^1]-octreotide in patients with neuroendocrine tumors. *J. Nucl. Med.* **2000**, *41*, 1514−1518.
(36) Froidevaux, S.; Eberle, A. N.; Christe, M.; Sumanovski, L.; Heppeler, A.; Schmitt, J. S.; Eisenwiener, K.; Beglinger, C.; Mäcke, H. R. Neuroendocrine tumor targeting: study of novel gallium-labeled somatostatin radiopeptides in a rat pancreatic tumor model. *Int. J. Cancer* **2002**, *98*, 930−937.
(37) Duncan J. R.; Stephenson, M. T.; Wu, H. P.; Anderson, C. J. Indium-111-diethylene-triaminepentaacetic acid-octreotide is delivered in vivo to pancreatic, tumor cell, renal, and hepatocyte lysosomes. *Cancer Res.* **1997**, *57* (4), 659−671.
(38) Bass, L. A.; Lanahan, M. V.; Duncan, J. R.; Erion, J. L.; Srinivasan, A.; Schmidt, M. A.; Anderson, C. J. Identification of the soluble in vivo metabolites of indium-111-diethy-lenetriaminepentaacetic acid-D-Phe1-octreotide. *Bioconjugate Chem.* **1998**, *9* (2), 192−200.
(39) Schottelius, M.; Wester, H. J.; Reubi, J. C.; Senekowitsch-Schmidtke, R.; Schwaiger, M. Improvement of pharmacokinetics of radioiodinated Tyr3-octreotide by conjugation with carbohydrates. *Bioconjugate Chem.* **2002**, *13* (5), 1021−1030.
(40) Wester, H. J.; Schottelius, M.; Scheidhauer, K.; Reubi, J. C.; Wolf, I.; Schwaiger, M. Comparison of radioiodinated TOC, TOCA and Mtr-TOCA: the effect of carbohydration on the pharmacokinetics. *Eur. J. Nucl. Med. Mol. Imaging* **2002**, *29* (1), 28−38.
(41) Vaidyanathan, G.; Friedman, H. S.; Schottelius, M.; Wester, H. J.; Zalutsky, M. R. Specific and high-level targeting of radiolabeled octreotide analogues to human medulloblastoma xenografts. *Clin. Cancer Res.* **2003**, *9* (5), 1868−1876.
(42) Schottelius, M.; Senekowitsch-Schmidtke, R.; Kessler, H.; Schwaiger, M.; Wester, H. J. First in-vivo data of [^{111}In]Maltose-Lys^0(DOTA)-Tyr^3-octreotide indicate a high potential of glycated, radiometalated octreotide derivatives for diagnosis and therapy. *Nucl. Med. Commun*. **2000**, *21*, 579 (abstract).
(43) Wester, H. J.; Schottelius, M.; Schwaiger, M. [^{99m}Tc](CO)$_3$-labeled carbohydrated SSTR-ligands: synthesis, internalisation kinetics and biodistribution on a rat pancreatic tumor model *J. Nucl. Med.* **2001**, *42* (Suppl.), 115P (abstract).
(44) Wester, H. J.; Schottelius, M.; Scheidhauer, K.; Meisetschläger, G.; Herz, M.; Rau, F.; Reubi, J. C.; Kimmich, T.; Arnold, W.; Schwaiger, M. PET imaging of somatostatin receptors: design, synthesis and preclinical evaluation of a novel ^{18}F-labelled, carbohydrated analogue of octreotide. *Eur. J. Nucl. Med.* **2003**, *30*, 117−122.
(45) Schottelius, M.; Poethko, T.; Herz, M.; Kessler, H.; Schwaiger, M.; Wester, H. J. First ^{18}F-labelled tracer suitable for routine clinical imaging of sst-receptor expressing tumors using positron emission tomography. *Clin. Cancer Res*. **2004**, *10*, 3593−3606.
(46) Funcke, W. ^{13}C NMR-Untersuchungen an Mutarotationsgemischen C-6- und C-4- sowie C-6-modifizierter Amadoriverbindungen. *Liebigs Ann. Chem.* **1978**, 2099−2104.
(47) Wester, H. J.; Schottelius, M.; Schwaiger, M. Glycation of sst-receptor-agonists: improvement of dynamic ligand trafficking of radiolabelled somatostatin analogs. *J. Labelled Compd. Radiopharm.* **2001**, *44* (Suppl. 1), S93.
(48) Reubi, J. C.; Schaer, J. C.; Waser, B.; Wenger, S.; Heppeler, A.; Schmitt, J. S.; Maecke, H. R. Affinity profiles for human somatostatin receptor subtypes SST1−SST5 of somatostatin radiotracers selected for scintigraphic and radiotherapeutic use. *Eur. J. Nucl. Med.* **2000**, *27*, 273−282.
(49) Hofland, L. J.; Breeman, W. A.; Krenning, E. P.; de Jong, M.; Waaijers, M.; van Koetsveld, P. M.; Mäcke, H. R.; Lamberts, S. W. Internalization of [DOTA^0,^{125}I-Tyr^3]octreotide by somatostatin receptor-positive cells in vitro and in vivo: implications for somatostatin receptor-targeted radioguided surgery. *Proc. Assoc. Am. Physicians* **1999**, *111*, 63−69.
(50) Albert, R.; Marbach, P.; Bauer, W.; Briner, U.; Fricker, G.; Bruns, C.; Pless, J. SDZ CO 611: a highly potent glycated analog of somatostatin with improved oral activity. *Life Sci.* **1993**, *53*, 517−525.
(51) Law, P. Y.; Maestri-El Kouhen, O.; Solberg, J.; Wang, W.; Erickson, L. J.; Loh, H. H. Deltorphin II-induced rapid desensitization of δ-opioid receptor requires both phosphorylation and internalization of the receptor. *J. Biol. Chem.* **2000**, *275*, 32057−32065.
(52) Marie, N.; Lecoq, I.; Jauzac, P.; Allouche, S. Differential sorting of human δ-opioid receptors after internalization by peptide and alkaloid agonists. *J. Biol. Chem.* **2003**, *278*, 22795−22804.
(53) Kokotos, G. A convenient one-pot conversion of N-protected amino acids and peptides into alcohols. *Synthesis* **1990**, 299−301.
(54) . Elofsson, M.; Walse, B.; Kihlberg, J. Building blocks for glycopeptide synthesis: Glycosylation of 3-mercaptopropionic acid and Fmoc-amino acids with unprotected carboxyl groups. *Tetrahedron Lett.* **1991**, *32*, 7613−7616.

JM040794I